

## Operating Characteristics of a 15-cm dia. Ion Engine for Small Planetary Spacecraft

John R. Brophy,\* Lewis C. Pless,\*\* Juergen Mueller,\*\* and John

*Jet Propulsion Laboratory  
California Institute of Technology  
Pasadena, California*

A 15-cm diameter, scaled-down version of the NASA light-weight 30-cm ion engine has been developed for potential application to very small planetary spacecraft. This engine has an active beam diameter of 150 mm, an outer ground screen diameter of 200 mm, and is 260 mm long. The engine mass is approximately 2.4 kg. This engine may be used as a stand-alone 15-cm engine, or it may be integrated into a segmented engine configuration to produce a 30-cm equivalent engine. It will also be used as a test bed for the development of advanced ion accelerator systems. The engine has been tested with two 3-grid accelerator systems, one with the electrodes fabricated from 0.38-mm thick molybdenum and the other fabricated from 0.51-mm thick graphite. Operation over an input power range of 380 to 1250 W and a specific impulse range of 2500 to 4000 s has been demonstrated. Preliminary measurements indicate that the performance is slightly better than projected over this specific impulse range. Operation with a negatively biased decelerator grid is shown to enable operation at net-to-total voltage ratios as high as 0.94.

### Introduction

Future planetary missions will require consideration of the entire life cycle mission costs including the cost of the launch vehicle. This has motivated program planners to consider means by which smaller, less expensive launch vehicles can be used to accomplish solar system exploration missions of interest. Solar electric propulsion with xenon ion engines provides enormous leverage to download planetary spacecraft to smaller launch vehicles through the large propellant mass savings characteristics of this technology. This trend to smaller launch vehicles is also accompanied by the planned development of smaller, less expensive, planetary spacecraft.<sup>1,2</sup> Total spacecraft dry masses of 300 kg (including the science instruments) or less are planned<sup>1,2</sup>. As the size of planetary spacecraft is decreased in order to get on smaller launch vehicles, the dry mass and physical size of ion propulsion systems to be used on these spacecraft must also decrease. The high efficiency, light-weight 30-cm diameter ion engine currently under development by NASA<sup>3</sup> may be larger than optimum for very small spacecraft under consideration.

This paper describes the first steps in the development of a 15-cm diameter xenon ion source. This source is being developed for three primary purposes. First, it may be useful in an ion propulsion system for a small spacecraft as a stand-alone, 15-cm xenon ion engine with a maximum input power (to the power processing unit) of 1.25 kW. Second, it may be integrated together with three other identical ion sources to produce a 4x15-cm segmented ion engine<sup>4</sup> with a maximum input power of 5.0 kW. Third, it may be used as a test bed for the development of advanced ion accelerator systems.

### Thruster Design

The 15-cm ion source represents essentially a scaled-down version of the NASA light-weight, 30-cm engine.<sup>3</sup> The two main discharge chamber components are fabricated from 1.6-mm thick 6061 aluminum sheets through the use of a spinning process. One component of the ground screen, which also serves as the structural support and engine mount is also spun from 6061 aluminum. The use of aluminum to minimize the mass of the ion source was first demonstrated by Patterson.<sup>3</sup>

The discharge chamber magnetic circuit is comprised of two rings of samarium-cobalt magnets, one positioned at the upstream end of the source near the cathode, and the other near the accelerator system. The magnet rings are attached to retaining rings machined from mild steel. The use of steel for these parts significantly simplifies assembly of the ion source without adding appreciably to the mass.

The main discharge chamber cathode design was

\*Supervisor, Advanced Propulsion Technology Group

\*\*Member of the Technical Staff, Electric Power Systems Section

\*\*\*Member of the Technical Staff, Advanced Propulsion Technology Group

similar to that tested for 5,000 hours<sup>5</sup> with the exception that the cartridge heater was replaced with a swaged heater. An enclosed keeper configuration was employed in the 15-cm ion source because it lends itself easily to a rugged structural design. The keeper electrode was fabricated from graphite to minimize fabrication costs and improve resistance to sputtering.

The accelerator system mounting ring is mounted to the downstream face of the magnet retaining ring at the downstream end of the discharge chamber. This was done to minimize the outside dimensions of the ion source. With this configuration, the outside diameter of the ion source ground screen is only 200 mm, while the diameter of the active grid area is 150 mm. This physically compact design has a significant effect on the overall size of the segmented ion engine configuration described in the next section. A schematic of the discharge chamber configuration is given in Fig. 1.

Initial testing of the ion source was performed using high pressure propellant isolators. Viscojets were used to drop the propellant pressure downstream of the isolators to the level required by the main discharge chamber and hollow cathode. These components were packaged at the rear of the ion source resulting in an overall source length of 260 mm (front ground screen to rear ground screen). Propellant flow rate control was achieved through the use of micrometer valves positioned outside of the vacuum chamber. This test configuration proved capable of standing-off the applied high voltages, but resulted in a very slow temporal response to changes in the micrometer valve settings in order to change the flow rate. This slow response is a result of the volume of propellant gas between the micrometer valves and the viscojets. Since the pressure of the gas in this volume is 2 to 4 orders of magnitude higher than in a low pressure feed system, the quantity of "trapped" propellant is substantial.

Subsequent testing was performed with a low pressure feed system to improve the response time. In this case high voltage isolation was provided through the use of 250-mm long pieces of elastomer tubing. Three pieces of 6-mm long boron nitride cylinders with 0.33-mm diameter holes drilled down the center were added to each length of tubing to prevent electrical breakdowns.

The neutralizer used for the tests to date consists only of a laboratory design originally used with a 30-cm thruster. No effort was made to minimize its mass or volume or to adjust its thermal characteristics for operation at the much lower emission currents required to neutralize the ion beam of the 15-cm engine. A compact, lightweight neutralizer has been designed by NASA LeRC<sup>3</sup> with a mass of only 115 g, so there was no need to duplicate this work.

The 15-cm ion source, including a three grid accelerator system, the ground screen and structural attachment points, but not including the neutralizer assembly, has a mass of

2.25 kg. This mass includes a 480-mm long wire harness. Adding to this 115 g for the neutralizer assembly of Ref. [3] results in a total mass of 2.36 kg if this ion source were to be used as a stand-alone, 15-cm ion engine.

### Testbed for Advanced Ion Optics

The key to improving ion engine endurance, reliability and performance is contained largely in the technology of the ion accelerator system. For this reason a variety of advanced grid technologies are being investigated including: the 3-grid SAND accelerator system,<sup>6</sup> carbon-carbon grids,<sup>7</sup> dished graphite grids, and grids fabricated from diamond films.<sup>8</sup> The 15-cm ion source will be used as a testbed for the evaluation of these candidate technologies. This should facilitate rapid, cost-effective accelerator system evaluation since it is easier and less expensive to fabricate grids in a 15-cm size as opposed to the 30-cm size. Promising candidates, such as the carbon-carbon grids will be fabricated and tested in a 30-cm size for possible application to the NASA lightweight 30-cm engine.

As of this writing the 15-cm engine has been tested with two accelerator systems with the characteristics given in Table 1. The "3-grid molybdenum" system consists of 3 molybdenum grids which were cut from the centers of the 3-grid accelerator system tested in Ref. [6]. These electrodes were isolated from each other through the use of 0.51-mm thick pieces of mica. The resulting assembly was held together and attached to the discharge chamber body with paper clips.

The "3-grid graphite" system consists of 3 dished graphite electrodes fabricated from ~~XXXXX~~ graphite. The spherically dished shaped grid was machined from a thick piece of graphite using a numerically controlled mill. The apertures in all three grids were mechanically drilled. The brittle nature of graphite made it impossible to fabricate the screen grid with the same open area fraction as the molybdenum screen grid. Consequently, the graphite screen grid was fabricated with a hole diameter of 1.78 mm rather than 1.91 mm, but with the same center-to-center hole spacing. The graphite grids were also made thicker to improve their mechanical strength. The dish depth was the same for both the molybdenum and graphite electrodes since the coefficient of thermal expansion for the graphite is very similar to that of molybdenum. A photograph of the dished graphite accelerator system is given in Fig. 2. The entire graphite accelerator system mass, including the grids, the mounting ring, insulators, screws and washers, is only 156 g. The grid to grid separation was 0.51 mm for both the screen-to-accelerator and accelerator-to-decelerator grids for the molybdenum electrodes. The screen-to-accelerator grid separation was 0.61 mm and the accelerator-to-decelerator grid gap was 0.51 mm for the graphite electrodes.

**Table 1 Grid Geometries**

Parameter	3-Grid Molybdenum Accelerator System	3-Grid Graphite Accelerator System
Screen Grid Thickness (mm)	0.381	0.508
Screen Grid Hole Diameter (mm)	1.91	1.78
Screen Grid Open Area Fraction	0.67	0.58
Screen-Accelerator Grid Separation (mm)	0.51	0.61
Accelerator Grid Thickness (mm)	0.381	0.508
Accelerator Grid Hole Diameter (mm)	1.14	1.50
Accelerator Grid Open Area Fraction	0.24	0.41
Accelerator-Deaccelerator Grid Separation (mm)	0.51	
Deaccelerator Grid Thickness (mm)	0.381	0.508
Deaccelerator Grid Hole Diameter (mm)	1.52	1.4
Deaccelerator Grid Open Area Fraction		0.47

**Preliminary Performance**

Preliminary measurements of the total engine efficiency as a function of specific impulse were obtained over the range of specific impulses from 2500 to 4000 s. These data were obtained with both the molybdenum and graphite accelerator systems. The total engine efficiency includes the neutralizer flow rate and keeper power. It does not, however, include approximately 50 W of heater power used to keep the neutralizer cathode sufficiently hot. As mentioned earlier, this neutralizer was originally used in tests with a 30-cm diameter thruster and was, therefore, sized to operate at higher emission currents than required for operation with the 15-cm thruster. The heater power was not included in the overall efficiency determination because with the proper thermal design the neutralizer cathode could easily be made to be self-heating.

The thruster efficiency was calculated from the appropriate electrical parameters measured during thruster operation. No direct thrust measurements were made. An approximate correction to the thrust calculation for beam divergence and multiply charged ions was applied by assuming the product of the corresponding thrust loss factors for these effects has a value of 0.95. Since Ibis is a very approximate procedure, the resulting uncertainty in thrust and specific impulse is relatively large. A correction for back-ingestion of propellant from the vacuum facility was also applied to the calculations of specific impulse and total efficiency. In the performance curves for beam ion production cost versus propellant efficiency, the propellant efficiency is also corrected for back-ingestion of propellant, but not for corrected for multiply charged ions.

The preliminary measurements for total engine efficiency are given in Fig. 3 for operation with both the molybdenum and graphite accelerator systems. The engine performance with the molybdenum grids is superior to that with the graphite grids as a result of the higher physical open area of the molybdenum screen grid. The solid line in the figure represents the performance projected for the

engine made several months before the engine was first tested. These performance projections were used in the mission analyses performed at JPL to compliment the NASA SEP Technology Applications Readiness (NSTAR) program.<sup>9</sup> The actual engine performance with the molybdenum grids is seen to be slightly better than the projected performance. These performance data were obtained with a variety of total propellant flow rates and input powers, and a discharge voltage of 30 V. The projected performance, however, assumed operation at a constant flow rate and beam current (of 500 mA).

The data of Fig. 3 for the molybdenum grids is repeated in Fig. 4 with error bars included to indicate the uncertainty in these quantities. As mentioned above the uncertainties are rather large, primarily as a result of the approximate thrust corrections for beam divergence and multiply charged ions. The error bars in Fig. 4 probably over estimate the uncertainty, but without a direct thrust measurement or measurements of the beam divergence and multiply charged ions it is impossible to reduce the uncertainty. The ability to perform direct thrust measurements is currently being implemented.

**Molybdenum Grids**

Data obtained for operation at a fixed beam current of 500 mA with the molybdenum accelerator system is given Fig. 5. These data were obtained by fixing the total propellant flow rate and varying the screen grid and accelerator grid voltages to vary the specific impulse. Slight adjustments ( $\leq 0.2$  A) to the discharge current were made to keep the beam current constant as the total voltage between the screen and accelerator grids was varied. The decelerator grid bias was set to -100 V relative to neutralizer common potential. The discharge voltage was constant (within 1%) at 30.3 V for these data. The solid line again gives the performance projected for the engine.

These data indicate that the engine can be operated over the range of input powers from 500 to 900 W at a constant

beam current of 500 mA. At specific impulses greater than 2900 s the accelerator grid voltage was maintained at -100 V. Below 2900 s greater negative voltages were required on the screen grid in order to extract the beam current. The variation of accelerator and decelerator grid currents versus total voltage is given in Fig. 6, indicating that direct ion impingement on the grids increases rapidly below a total voltage of 1040 V for a beam current of 500 mA. At the minimum input power point of 5(N) W, the specific impulse was 2670 s corresponding to a net accelerating voltage of 750 V. At this operating point the magnitude of the accelerator grid voltage reached its maximum value (300 V).

The discharge chamber performance is given in Fig. 7 for the operation with the molybdenum and graphite grid systems at a constant discharge voltage of 30 V and a constant total discharge chamber propellant flow rate (including back-ingestion) of approximately 0.66 mg/s. (The cathode flow rate was adjusted to maintain the discharge voltage constant over the performance curve, resulting in a slight variation in discharge chamber total flow rate). Again, the performance with the molybdenum grids is significantly better than that with the graphite due to the higher open area fraction for the molybdenum grids. It is clear from these data that the discharge propellant utilization has not been corrected for multiply charged ions as evident from the values of this parameter which approach unity.

The discharge chamber performance for operation at a discharge voltage of 28 V and a total discharge chamber propellant flow rate of approximately 0.79 mg/s is given in Fig. 8. These data indicate acceptable discharge chamber performance even at a discharge voltage of 28 V with the molybdenum grids.

### Graphite Grids

The discharge chamber performance for operation with the graphite accelerator system is given in Fig. 9 for two different discharge chamber propellant flow rates. The effect of increasing flow rate has the expected effect of reducing the beam ion production cost for a given propellant efficiency.<sup>10</sup>

The performance characteristics of the graphite grids is given in Fig. 10 for a beam current of 400 mA. These data indicate that a total voltage of approximately 12(M) V is required to extract the beam current of 400 mA. This is in contrast to the molybdenum grids where a beam current of 500 mA could be extracted with a total voltage as low as 1040 V. The superior performance of the molybdenum grids is most likely due to the smaller grid separation used with these grids (see Table 1).

The effect of decelerator grid voltage on electron back streaming is given in Fig. 11 for the graphite grids. With 110 decelerator grid voltage (i.e., the decelerator grid at neutralizer common potential) the magnitude of the negative accelerator grid voltage must be at least 260 V to prevent

electron back streaming. The magnitude of the accelerator grid voltage required to prevent electron back streaming is reduced to approximately 200 V when the decelerator grid is biased to -50 V. With -104 V on the decelerator grid, the accelerator grid voltage could be reduced to -104 V and still prevent electron back streaming. The magnitude of the accelerator grid voltage was not reduced below the magnitude of the decelerator grid voltage.

For these data the neutralizer coupling voltage was approximately 30 V. Therefore, with -100 V applied to both the accelerator and decelerator grids, the maximum incident charge exchange ion energy is 130 eV. The sputter yield of graphite for incident xenon ions with 130 eV of energy is approximately 0.01 atoms/ion.<sup>11</sup> The nominal 2.3 kW operating point for the 30-cm ion engine to be used in the NSTAR technology validation program, the accelerator grid voltage is -150 V [Patterson 2-1993]. Assuming a neutralizer coupling voltage of 20 V, the maximum energy of charge exchange ions striking the accelerator grid is 170 eV. The sputter yield for xenon on molybdenum<sup>11</sup> at this energy is approximately 0.2?, which is more than a factor of 20 greater than the sputter yield for the graphite at 130 eV. The significance of this will be discussed in the following section on the segmented ion engine.

### Segmented Ion Engine

The segmented ion engine configuration described in Ref. [4] divides a large engine into several identical smaller ion sources configured to have the same active grid area as the original larger ion source. For example, a 5-kW, 30-cm diameter ion engine may be replaced by a segmented ion engine consisting of four 15-cm diameter ion sources in the manner shown in Fig. 12. These four ion sources (or segments) are operated from a single power conditioning unit in as suggested in Fig. 13. The chief advantage of doing this results from the requirement that the engine must operate over a large input power variation and that it must be capable of operating for typically 8,000(M) hours if this engine is used in an SEP system for a planetary spacecraft. The segmented engine is throttled primarily by shutting off the individual 15-cm ion source segments. Power is removed from a segment and that segment is electrically isolated from the high voltage power supplies through the use of solid state switches. Propellant flow to that segment is also halted by closing the appropriate valve in the propellant feed system. For the segmented ion engine consisting of four 15-cm diameter ion sources, throttling the engine in this way enables a 4 to 1 input power variation. Finer throttling control is achieved by varying the net accelerating voltage at constant beam current as shown in Fig. 5 for a single ion source. This results in an overall throttling range as great as 7 to 1 for the 4x 15-cm segmented ion engine with constant propellant flow rate to each operating segment.

The major advantage in throttling the segmented ion engine in this manner is that the segments which have been

shut-off are no longer subject to wear. This results in a substantial reduction in the required service life of the ion source components for missions of interest such as comet and main belt asteroid rendezvous.

#### 4x15-cm Segmented Ion Engine

For the segmented ion engine comprised of four 15-cm ion sources and shown schematically in Fig. 12 the four ion sources are arranged in a square configuration with a single neutralizer cathode in the center. All of the ion sources are enclosed within a common ground screen. The sum of the four ion sources results in a total active beam area of  $707 \text{ cm}^2$  which is 13 % larger than the 30-cm engine<sup>3</sup> (which has an active beam diameter of 28.2 cm). This is packaged to fit within a frontal area which is nearly identical to that of the 30-cm engine as illustrated in Fig. 12. Packaging the 4x15-cm segmented engine into the same footprint as the 30-cm engine required that the ratio of outer diameter to active beam diameter for each individual 15-cm source be maintained equal to that of the 30-cm engine. This challenge was met by mounting the accelerator system "on top of" the downstream magnet ring, rather than adjacent to it as in conventional designs. The basic 15-cm discharge chamber without the ground screen, and wiring harness weighs less than 1.5 kg. The 4x15-cm segmented engine is currently being fabricated and is expected to weigh approximately 8 kg when completed.

Based on the performance data from Fig. 5 for a single 15-cm diameter ion source, the performance of the 4x15-cm segmented ion engine can be projected by multiplying the input power, and thrust by factors of 2, 3, and 4 corresponding to operation of 2, 3, and 4 ion sources in the segmented engine. The results of doing this are given in Fig. 14, where the projected thrust and specific impulse are given as functions of the total engine input power. The four curves in each graph refer to the number of operating segments. These data indicate a 1-to-1 input power throttling range (500 w to 3500 w). This was accomplished with each individual segment operated at a constant beam current of 500 mA. The power throttling range is continuous with the exception of a gap which occurs at input powers between 900 and 1000 w. This occurs because the range for throttling an individual 15-cm ion source at constant beam current does not quite cover a 2-to-1 power variation (its actually 1.8-to-1).

The baseline operating point for the 30-cm ion engine for the NSTAR technology validation program is an input power of 2.3 kW with a beam current of 1.8 A and a thrust level of 95 mN at a specific impulse of 3300 s. The projected performance of the 4x15-cm segmented engine at an input power of 2.4 kW and a beam current of 2.0 A is a thrust of 95 mN at a specific impulse of 3000 s. Furthermore, this performance can be achieved using the 3-grid SAN 10<sup>6</sup> accelerator system configuration, which enables operation with an accelerator grid voltage of only -100 V.

Furthermore, with the use of carbon-carbon electrodes currently under fabrication the expected sputter yield for charge-exchange ions may be more than a factor of 20 less than for a molybdenum accelerator grid operated at 150 V. This would completely remove accelerator grid erosion as a potential life-limiting mechanism for the ion engine.

#### Conclusions

A 15-cm diameter, scaled-down version of the NASA light-weight 30-cm ion engine has been developed for potential application to very small planetary spacecraft. As a stand alone 15-cm engine, the engine mass is approximately 2.4 kg, the active beam diameter is 150 mm and the outer diameter of the screen grid is only 200 mm. The engine has been operated over a specific impulse and input power range of 2500 to 4000 s and 380 to 1250 W, respectively. At a constant beam current of 500 mA, engine operation over an input power range of 500 to 890 W (corresponding to a specific impulse range of 2700 to 3900 s) was demonstrated. Applying a negative bias of -100 V to the decelerator grid of a 3-grid accelerator system enabled operation at accelerator grid voltages as low as -100 V for applied screen grid voltages of 1500 V (giving a net-to-total voltage ratio of 0.94). The use of carbon grids (carbon-carbon, dished graphite, or doped diamond films) at an accelerator grid voltage of -100 V is expected to completely eliminate accelerator grid erosion as a significant life-limiting mechanism.

Integration of the 15-cm ion source into 4x15-cm segmented engine configuration results in a 30-cm equivalent engine which can be throttled over a 7-to-1 input power variation with a constant beam current in each of the four segments. Throttling the segmented engine by turning off individual segments can result in a significant decrease in the required service life (and qualification requirements) of the ion source components.

#### Acknowledgments

The authors thank Mr. Alison Owens and Mr. William Thogmartin for fabricating the ion engine described herein and responding rapidly to configuration changes and facility problems.

The work described in this paper was performed by the Jet Propulsion Laboratory, California Institute of Technology, under contract with the National Aeronautics and Space Administration.

#### References

<sup>1</sup>Personal communication, Joel C. Serceel, Manager, Spacecraft Technology Demonstrations and Coordination, Jet Propulsion Laboratory, California Institute of Technology.

<sup>2</sup>Wallace, R. A., "Updated 2017 Mission Summary

Descriptions," JPI, IOM 312/92.3-5044, November 13, 1992, internal document.

<sup>3</sup>Patterson, M. J., Haag, W., and Williams, G. J., Jr., "Derated Ion Thruster Development Status," AIAA-92-3335, presented at the 29th Joint Propulsion Conference, Monterey, Jun 3, 1993.

<sup>4</sup>Brophy, J. R., "A Segmented Ion Engine Design for Solar Electric Propulsion Systems," AIAA-92-0608, presented at the 43rd Congress of the International Astronautical Federation, Washington, DC, August, 1992.

<sup>5</sup>Brophy, J. R., and Garner, C. E., "A 5,000 Hour Xenon Hollow Cathode Life Test," AIAA-91-122, presented at the 27th Joint Propulsion Conference, Sacramento, CA, June, 1991.

<sup>6</sup>Brophy, J. R., Pless, L. C., and Garner, C. E., "Ion Engine Endurance Testing at High Background Pressures," AIAA-92-3205, presented at the 28th Joint Propulsion Conference, Nashville, TN, July, 1992.

<sup>7</sup>Mueller, J., Brown, K., Garner, C., and Brophy, J. R., "Fabrication of 1.5-cm-dia. Carbon-Carbon Grids," IIP-93-117, presented at the 23rd International Electric Propulsion Conference, Seattle, WA, September, 1993.

<sup>8</sup>Personal Communication, John J. Blandino, Advanced Propulsion Technology Group, Jet Propulsion Laboratory, California Institute of Technology.

<sup>9</sup>Yen, C. L., and Sauer, C. G., "Applications of  $\Delta I$  (7925)/S1 IP to Mainbelt Asteroid Rendezvous Missions," JPI, IOM 312/93.3-5087, April 20, 1993, Jet Propulsion Laboratory internal document.

<sup>10</sup>Brophy, J. R., "Ion Thruster Performance Model, NASA CR-174810, December 1984.

<sup>11</sup>Matsunami, N., et al., "Energy Dependence of the Yields of Ion-Induced Sputtering of Monatomic Solids," IIP-AM-32, September 1983.

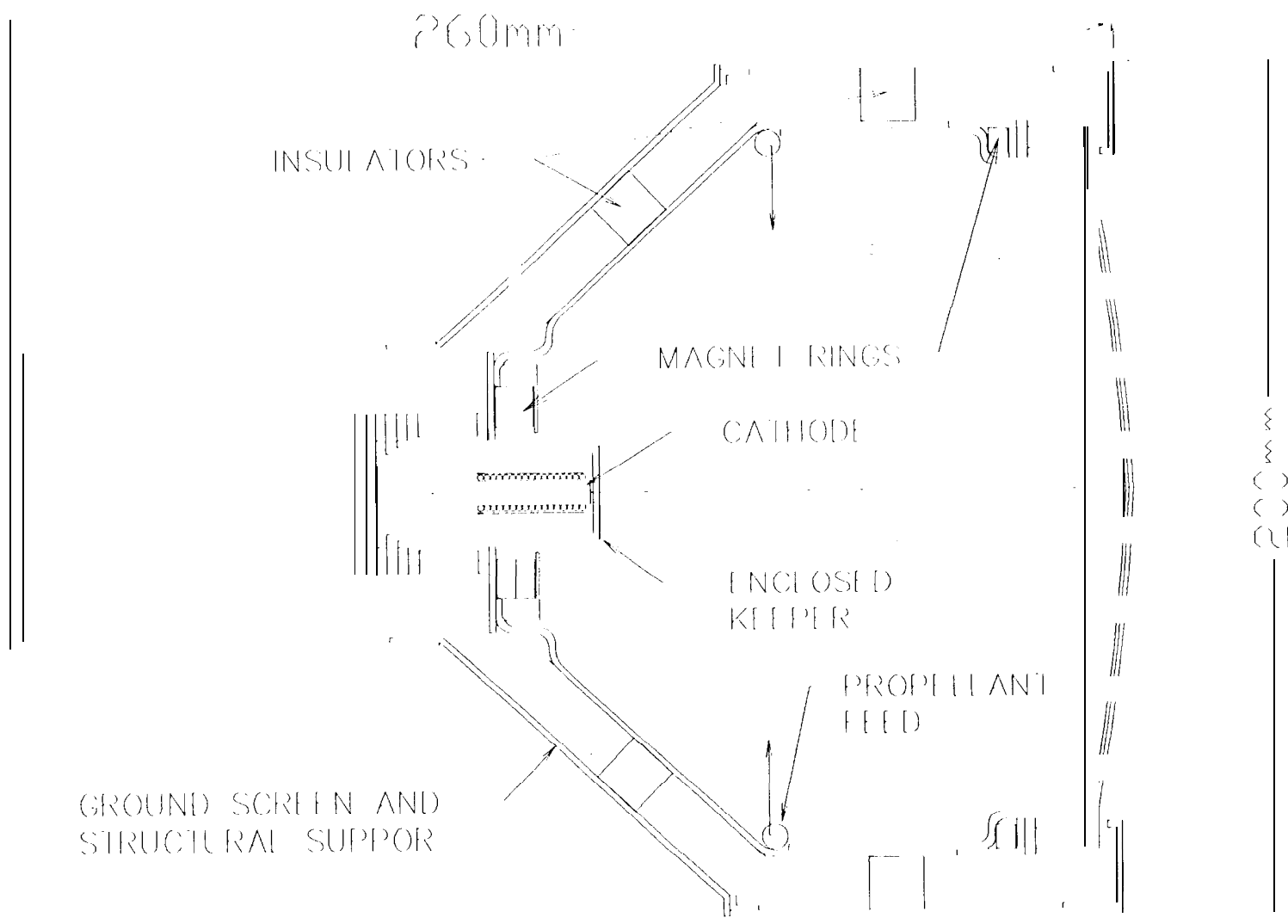


Fig. 1

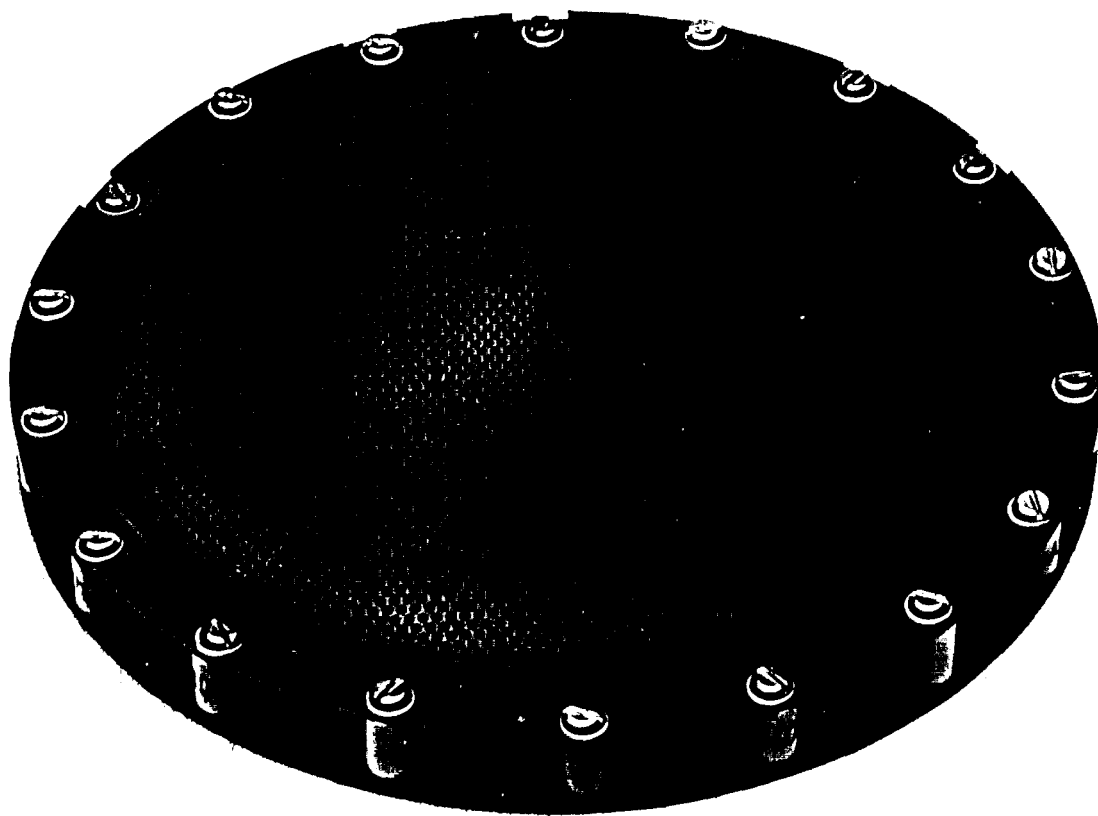


Fig. 2

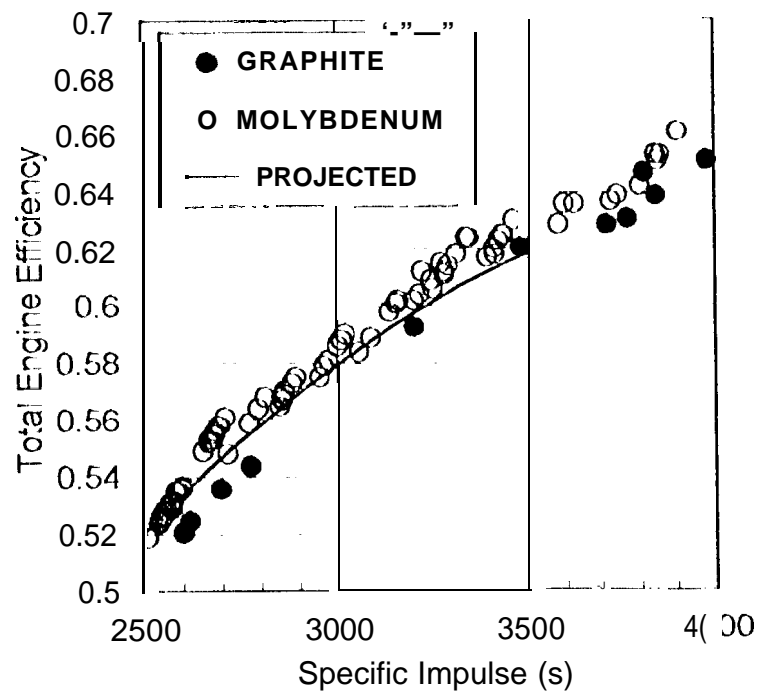


Fig. 3

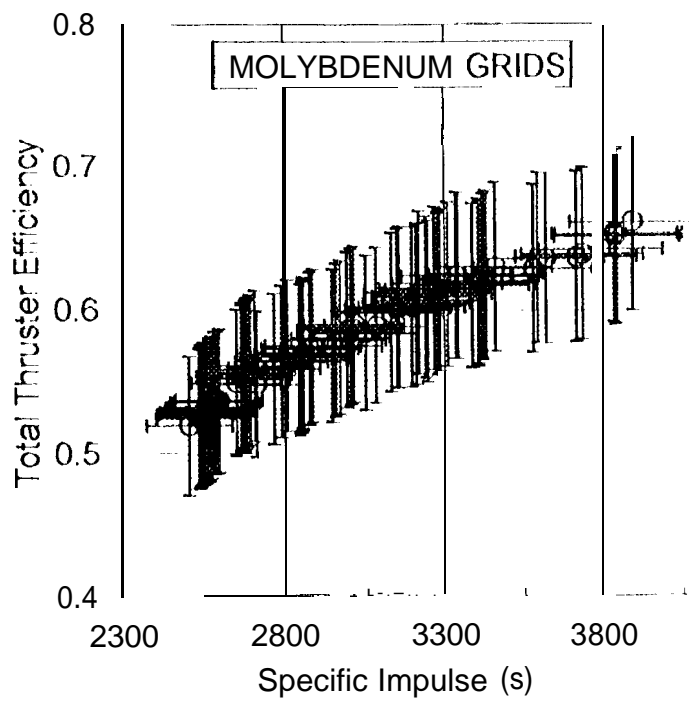


Fig. 264

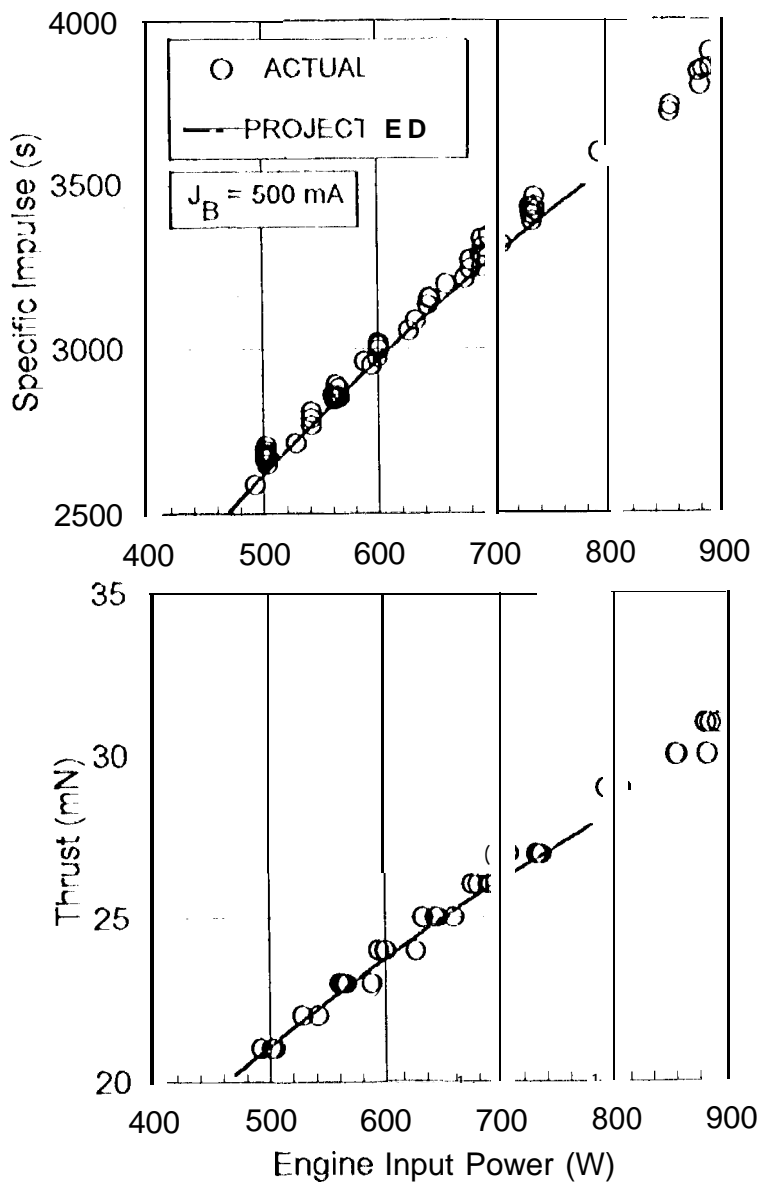
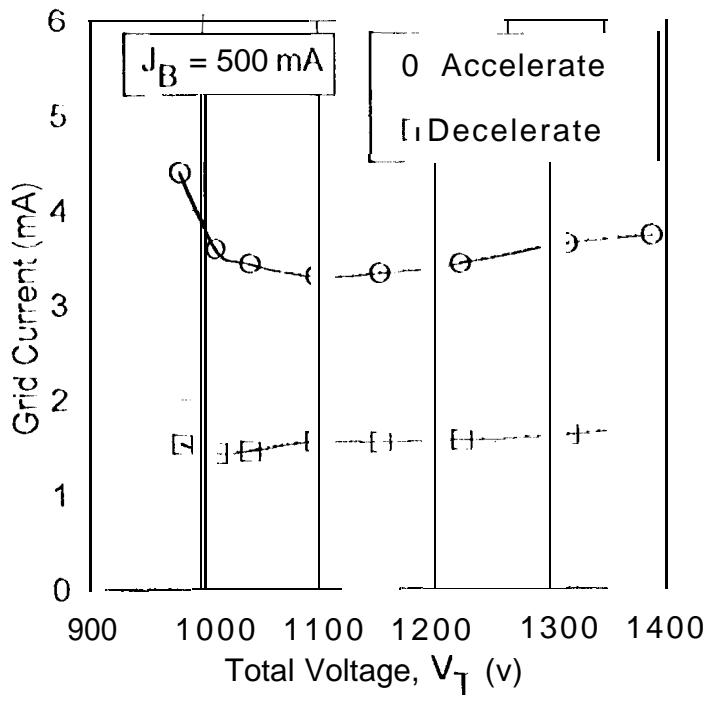


Fig. ~~158~~ 5



*Handwritten notes and arrows:*  
 A large downward-pointing arrow is on the left. To its right, the text "3.8 mA" is written in a cursive script.

Fig. ~~28~~ 6  
 Molybdenum

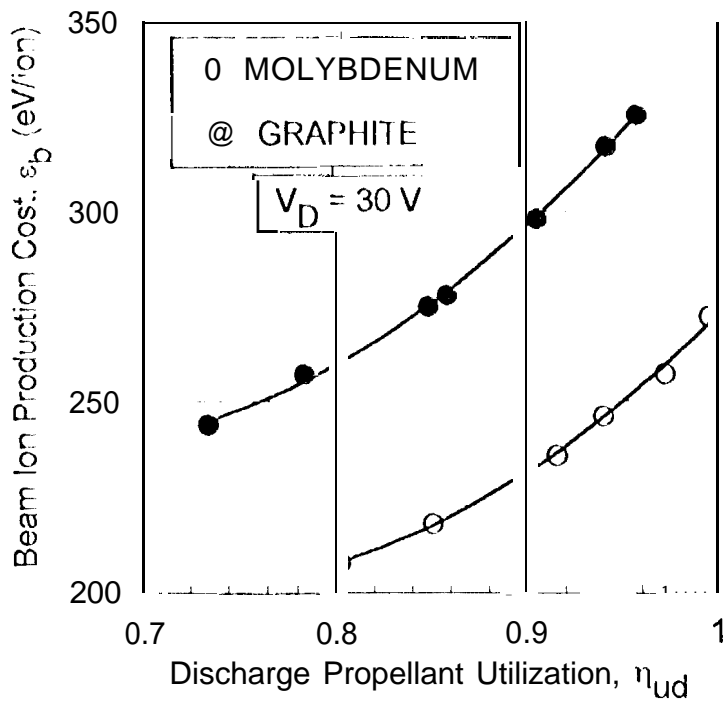


Fig. ~~809~~ 7

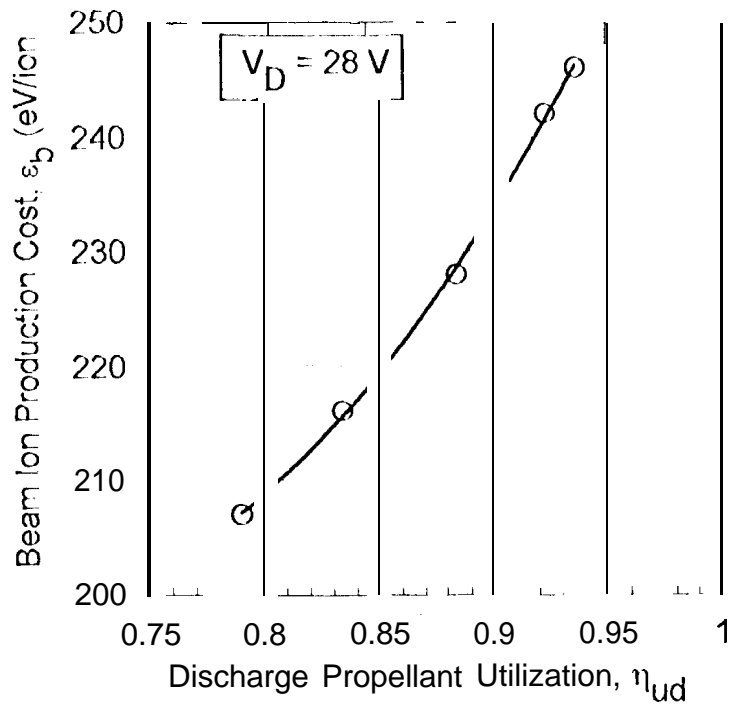


Fig. ~~7~~ 8

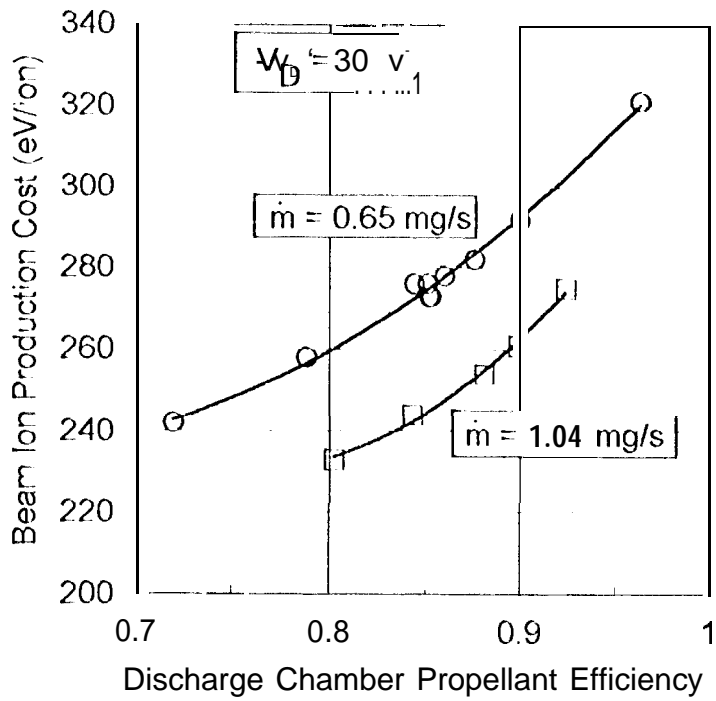
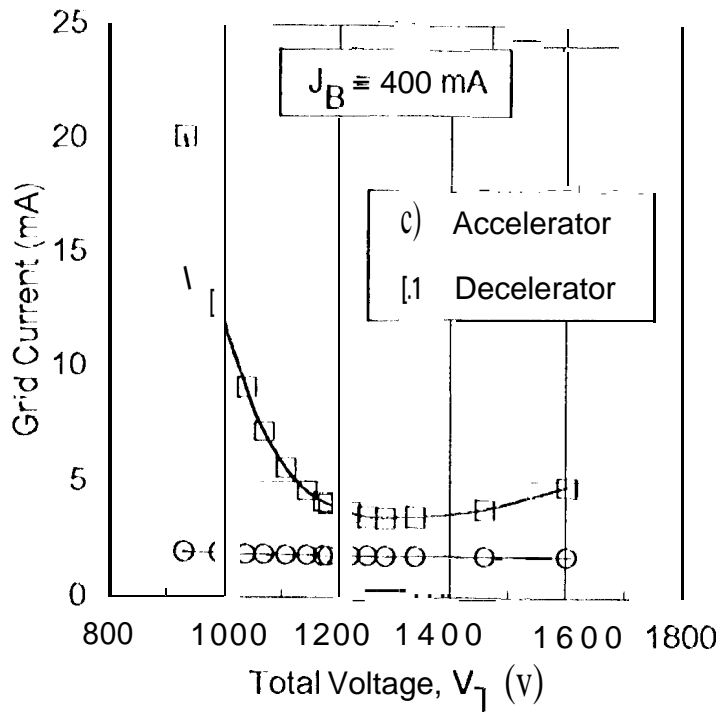


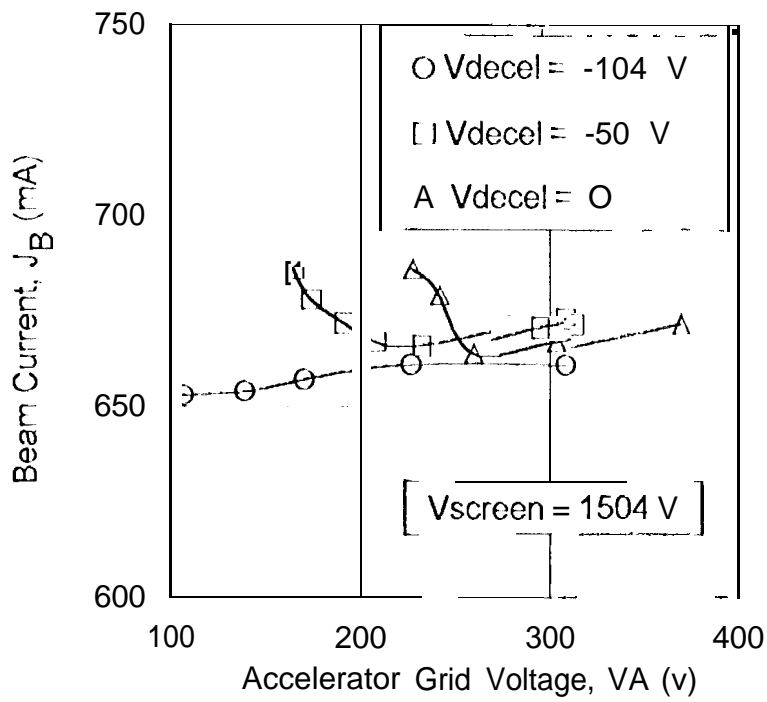
Fig. ~~10~~ 9

Graphite

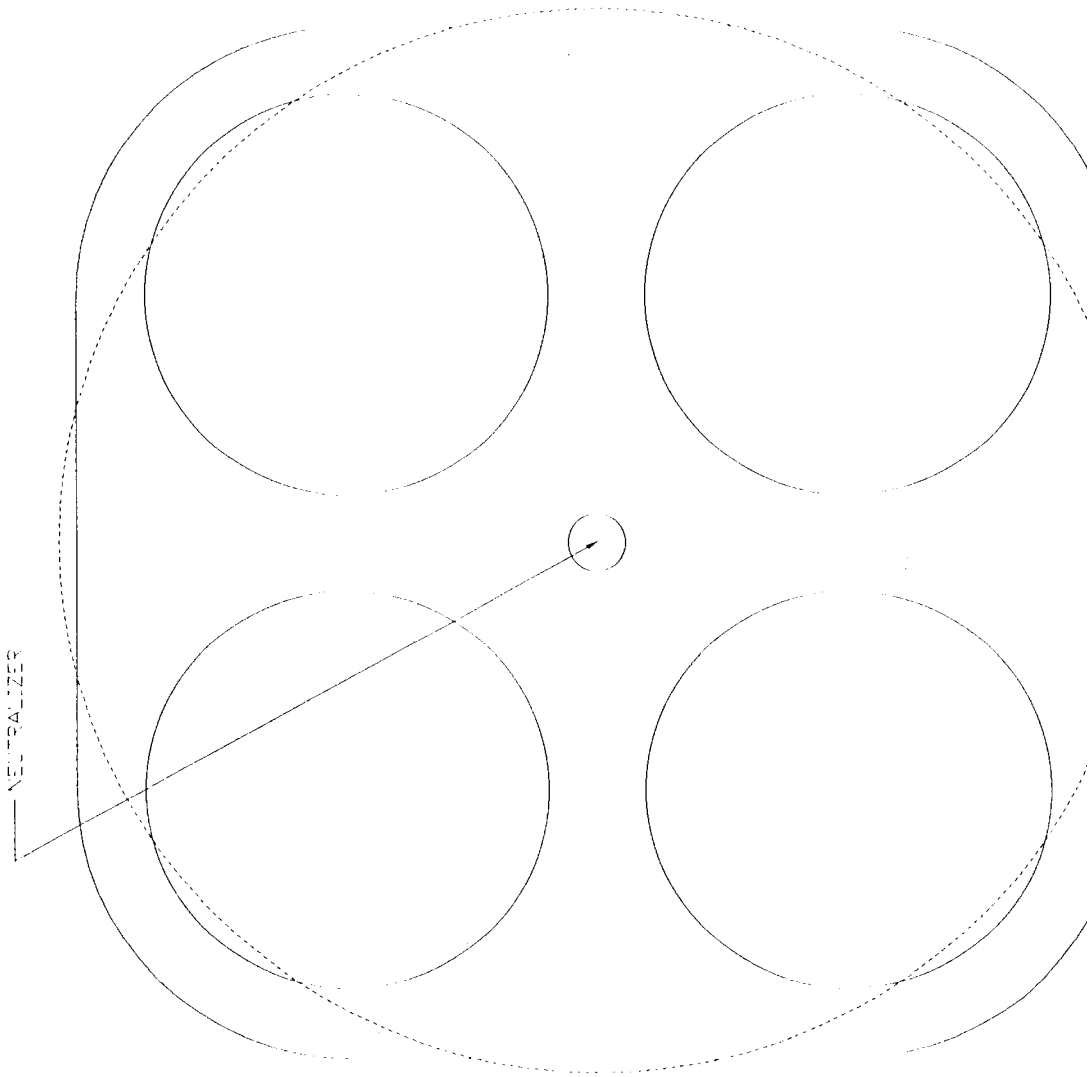


*Discontinued?*

Graphite Fig. ~~10~~ 10



Graphite... Fig. ~~4244~~ 11



GROUND SCREEN ENVELOPE FOR  
CONVENTIONAL 30-CV ENGINE

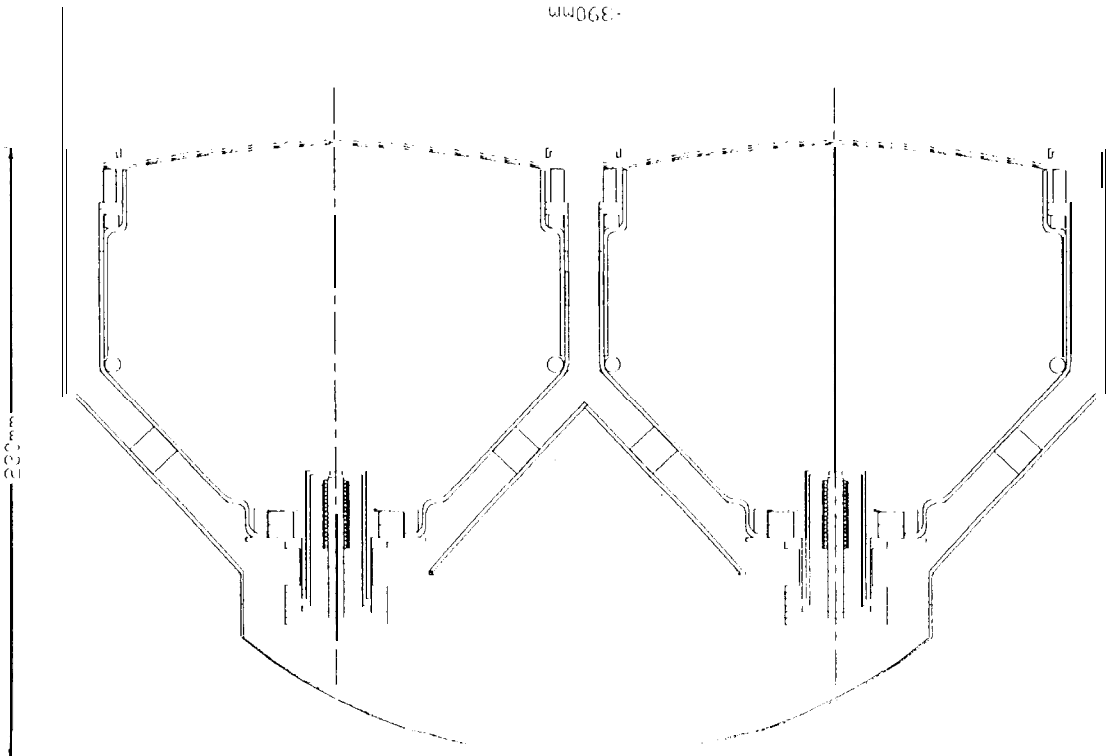


Fig 13

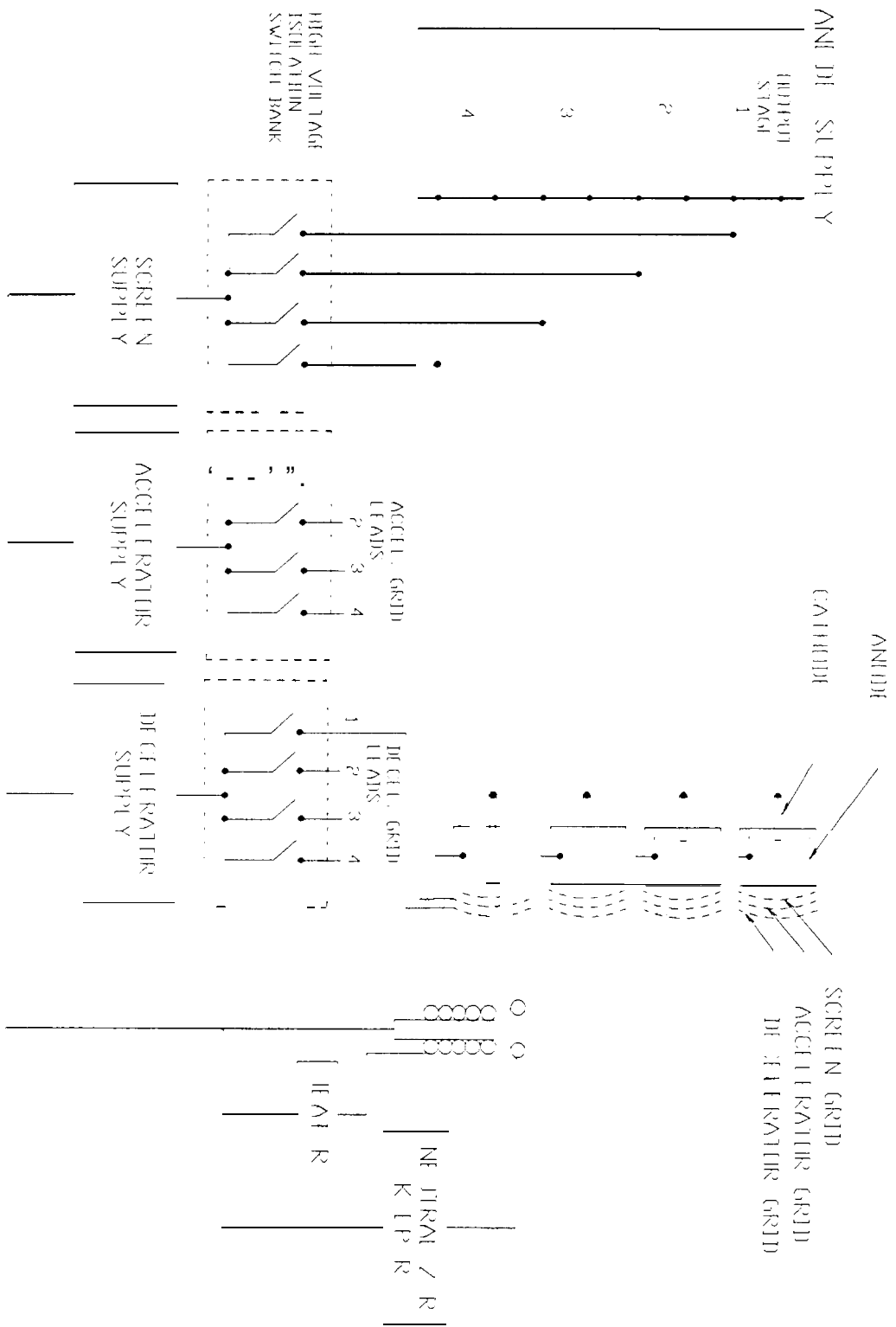


Fig. 13

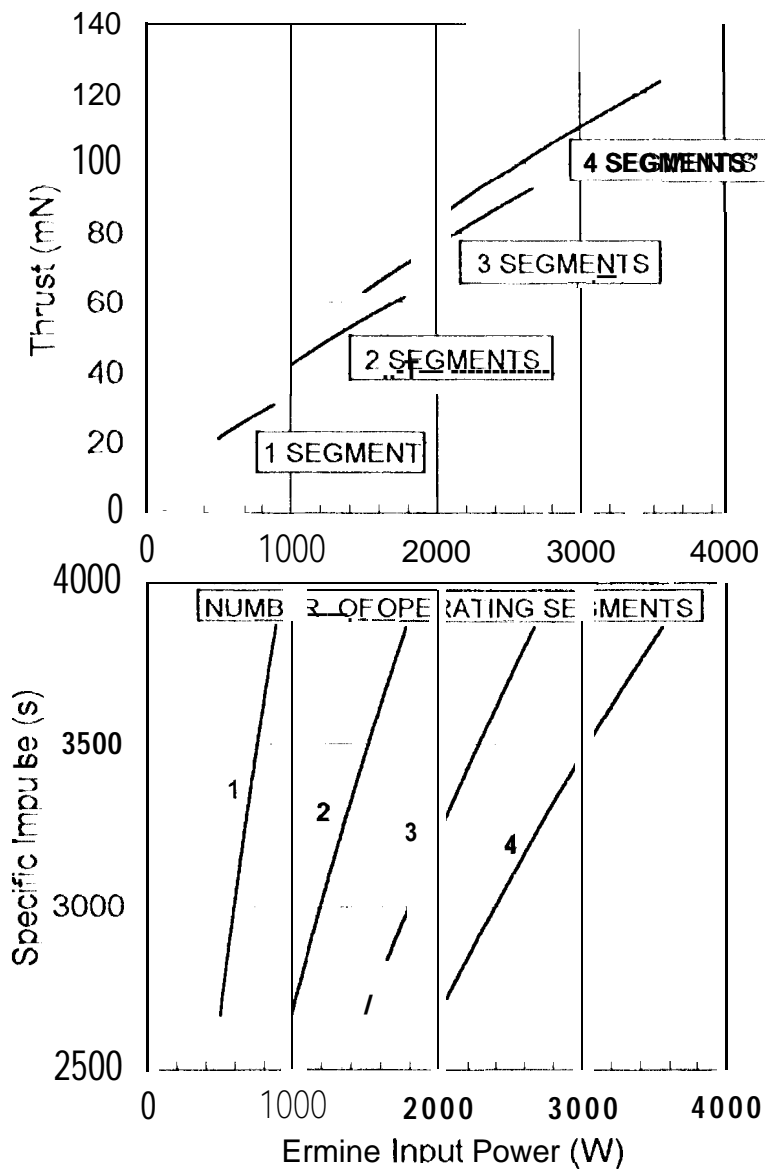


Fig. ~~1053~~ 14